Photoelectrochemical Approach for Metal Corrosion Prevention Using a Semiconductor Photoanode

Hyunwoong Park,[†] Kyoo Young Kim,[‡] and Wonyong Choi*[,†]

School of Environmental Science and Engineering and Department of Materials Science and Engineering, Pohang University of Science and Technology, Pohang, Korea 790-784

Received: January 15, 2002; In Final Form: March 8, 2002

Metal corrosion was successfully prevented using a TiO_2-based photoelectrochemical system. Under UV illumination, a TiO_2 electrode in a hole scavenging medium supplied photogenerated conduction band electrons to an electrically connected steel electrode with the generation of photocurrent and shifted the coupled potential to much more negative values. In this galvanic pair, the steel and the TiO_2 electrode acted as a cathode and a photoanode, respectively, which is essentially a variation of cathodic protection. The performance of the photocathodic protection depended little on the light intensity as long as there were enough photons to compensate for the dark corrosion current of the steel. The shiny surface of the steel electrode remained intact in a corrosive electrolyte solution as long as it was connected to the UV-illuminated TiO_2 photoanode, but it quickly corroded and was covered by red-brown rust in the absence of light. An outdoor test under solar light also showed a similar effect of corrosion prevention, which verified the possibility of using solar light for corrosion prevention. Although formate was useful as a hole scavenger, pure water without any added hole scavenger was also successful in protecting metal. The performance of the ZnO photoanode was similar to that of TiO_2. Various experimental parameters affecting the new photocathodic protection system were investigated and are discussed.

Introduction

Semiconductor photochemistry has been a topic of intensive study in many areas such as water splitting for solar energy conversion,[1] dye-sensitized solar cells,[2] environmental remediation,[3] and coating materials for photoinduced superhydrophilicity.[4] Recently, a few studies have proposed that the photoinduced charge-transfer process at the semiconductor interface can be applied to metal corrosion prevention. It has been found by chance in a study of the TiO_2 photocatalytic reaction that the preoxidized surface of the stainless steel plate used as a TiO_2 film support was reduced and bleached during illumination,[5] which indicated that the photogenerated conduction band (CB) electrons on the TiO_2-coated side (front) transferred to the back preoxidized surface through the metal bulk to induce reductive bleaching. Yuan and Tsujikawa[6] also reported that the potential of a TiO_2-coated copper substrate drastically shifted toward the negative direction under illumination. Accordingly, Fujishima and co-workers[7,8] have recently reported that the TiO_2-coated stainless steel plate showed an anticorrosion effect under UV illumination. These findings gave us the idea to use a semiconductor photoanode connected to a steel electrode as a new type of cathodic protection, which has been recently reported in a preliminary form.[9]

The basic strategy of cathodic protection is to supply the metal to be protected with enough electrons to shift its potential to the corrosion immunity region.[10] The source of electrons could be an external power supply or a sacrificial anode. The external power supply provides impressed current to metal through a rectifier by converting alternating current (AC) to direct current (DC). Usual sacrificial anodes such as Mg, Zn, and Al have more negative reduction potentials than does the metal to be protected, and thus the anode protects the metal by continually consuming itself through anodic dissolution and should be replaced periodically.[10] The cathodic protection system that uses no external power or no sacrificial anode has yet to be developed.

The basic idea of the present photocathodic protection method is to replace the sacrificial anode with a semiconductor photoanode that generates CB electrons upon band-gap irradiation, as shown schematically in Figure 1a. The photoelectrochemical system consisted of a simple TiO_2 photoanode, an electrically connected steel electrode, and a salt bridge connecting two compartment cells. Although the basic features of the present system are those of a typical photoelectrochemical cell in which the photoinduced electron transfer processes at the semiconductor/electrolyte interface (photoanode) are of major interest, this photoelectrochemical study for cathodic protection mainly deals with the photoeffects on the cathode (i.e., steel) material itself, not the photoanode.

In this work, the behavior of the photoelectrochemical cell used for the cathodic protection of the metal electrode was investigated in detail. Various experimental parameters related to the semiconductor (TiO_2 or ZnO), metal (steel) electrode, and the hole scavenger were systematically varied to describe the behavior of the system quantitatively and to assess its applicability as an alternative corrosion prevention method using solar light.

Experimental Section

Preparation of Electrodes. TiO_2 powder (Degussa P25) used for the semiconductor photoanode was known to be a mixture of ca. 30% rutile and 70% anatase (BET surface area = 55 m^2 g^{-1}), and ZnO powder was obtained from Aldrich. TiO_2 was

* To whom correspondence should be addressed. E-mail: wchoi@postech.ac.kr.
[†] School of Environmental Science and Engineering.
[‡] Department of Materials Science and Engineering.

10.1021/jp025519r CCC: $22.00
Published on Web 04/06/2002

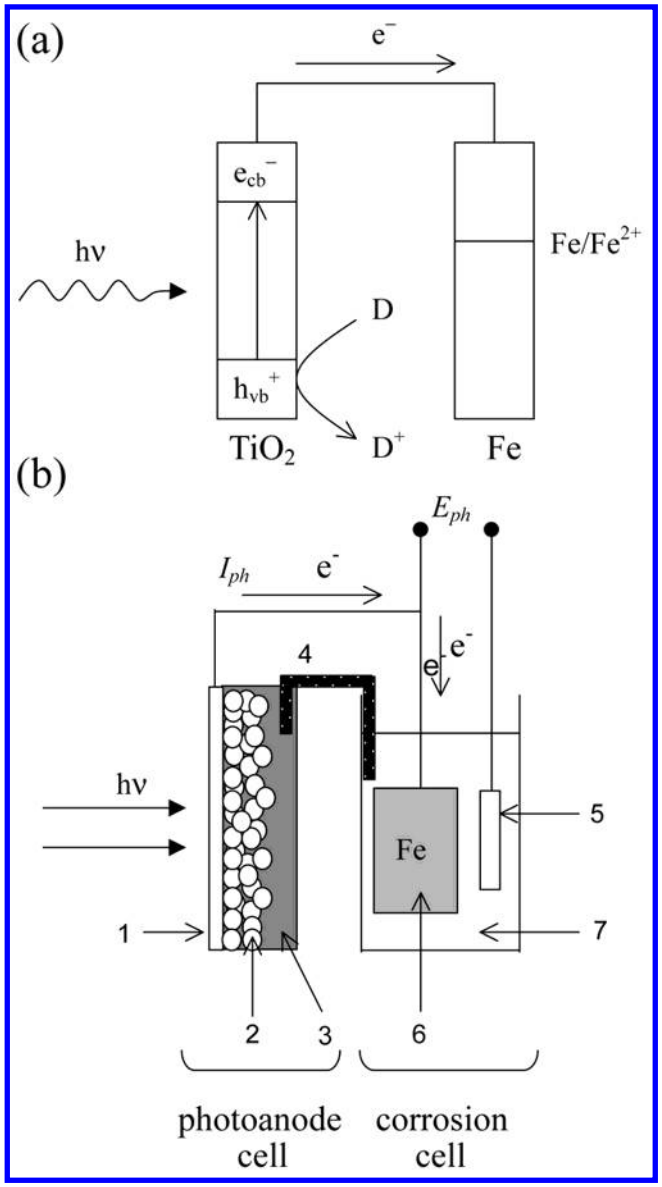

Figure 1. (a) Schematic representation of the photoelectrochemical metal corrosion prevention system using a TiO_2 photoanode. D represents a hole scavenger (electron donor). (b) Experimental setup of the photoelectrochemical cell for steel corrosion prevention. The major components are (1) ITO glass, (2) TiO_2 film (3) hole-scavenging medium containing formate (in aqueous solution or agar gel) or pure water, (4) salt bridge, (5) SCE, (6) steel electrode, and (7) electrolyte solution.

suspended in distilled water to produce a 5 wt % concentration, and the solution was sonicated for 10 min and mixed well. An ITO (indium tin oxide) glass plate (Delta Technologies, 7 × 5 cm^2, 10 Ω/square) was cleaned by sonicating in detergent solution for 30 min to remove organic contaminants. Four milliliters of the powdered suspension was spread over the ITO plate, and then the excess suspension was removed from the plate. The TiO_2/ITO electrode with a coating area of 14.8 cm^2 was dried in air for 1 h and heated at 450 °C for 30 min. The above processes were repeated when a thicker coating was needed. The TiO_2 coating thickness was measured by scanning electron micrographic analysis and was about 10 μm for a typical photoanode. Electrical contact to the TiO_2 electrode was made by attaching copper wire with silver paste at the uncoated edge of the ITO plate. The ZnO/ITO electrode was prepared in a similar way. A circular carbon steel electrode (surface area 1.66 cm^2) was mechanically polished with SiC emery paper, rinsed with acetone, and dried under air. The back and edges of the steel electrode were covered with epoxy resin to expose only the front surface to the electrolyte solution.

Photoelectrochemical Test. The photoelectrochemical setup consisted of two compartments: one for the TiO_2 photoanode and the other for the carbon steel electrode (cathode) immersed in an aqueous solution, as shown in Figure 1b. The two electrodes were galvanically coupled through an external circuit, and the two cells were connected by a salt bridge (flexible Tygon tubing containing saturated KCl in agar) to complete the circuit. The photoanode compartment contained the TiO_2/ITO electrode in the hole scavenging medium. Several organic alcohols and acids were tested as a hole scavenger in the photoanode cell, and sodium formate was used in most experiments. Two types of hole scavenging media containing formate were employed in this study: formate in aqueous solution or in agar gel. The performance of the photoanode showed little difference between the aqueous and gel media. The photoanode cell containing the aqueous formate solution had a Pyrex window to transmit UV light with $\lambda > 300$ nm. As for the one with agar gel, the TiO_2/ITO electrode was placed in gel containing formate solution (1 M) and was incased in a transparent Petri dish to form a flat solar cell. Pure distilled water was also tested as a hole scavenger. A small amount of hydrogen peroxide, which was analyzed by the DPD (*N*,*N*-diethyl-*p*-phenylenediamine) method according to a literature procedure[11], was produced in the photoanode cell as a result of water oxidation. Electrolytes in the corrosion cell were K_2CO_3 or NaCl.

The UV light source was three 10-W black-light lamps or a 200-W Hg lamp. The TiO_2/ITO electrode was illuminated from the ITO side. The UV intensities ($300 < \lambda < 400$ nm) that can excite the TiO_2 photoanode were measured to be 58, 100, and 130 $\mu W/cm^2$ and 1.54 mW/cm^2 for 10, 20, 30, and 200-W lamps, respectively. The intensities of UV light were measured using a power meter (Newport 1815C) equipped with a silicon diode detector. Photopotentials against SCE (saturated calomel electrode) and photocurrents were measured simultaneously by a potentiostat (EG&G, model 263A) that was connected to a computer. All electrochemical measurements were obtained using the galvanic corrosion mode in the M 352 program that was supplied by EG&G. The potentiostat that runs the galvanic corrosion experiment with SoftCorr III software in effect functioned as a zero-resistance ammeter.

Characterization of the Steel Electrode Surface. To analyze the corroded surface of the carbon steel immersed in electrolytes, a Raman spectrometer (Renishaw system 3000) was employed. It consisted of a microscope, a single spectrograph fitted with holographic notch filters for spectroscopy mode, and a Peltier-cooled CCD detector (600 × 800 pixels). The excitation wavelength was the 632.8-nm line of He−Ne laser. All Raman measurements were carried out with backscattering geometry, and almost all Rayleigh scattering was eliminated. Spectra were collected from five different spots on the steel surface and were averaged.

Results and Discussion

Optimization of Photoanode. When the TiO_2 electrode was connected galvanically to the steel electrode in the absence of illumination, the TiO_2 and steel electrodes were each cathodically or anodically polarized becaue of the difference of the open circuit potentials ($E_{oc,\ dark}(TiO_2) \approx 0$ vs $E_{corr}(\text{steel}) \approx -0.3 \pm 0.1$ V_{SCE}). In this case, the coupled potential was close to E_{corr}(steel) with minute electron flow (<1 μA) from the steel to the TiO_2 electrode. When the TiO_2 electrode was illuminated with UV light, it became more active (negative) than the steel because the photogenerated CB electrons transferred to the steel

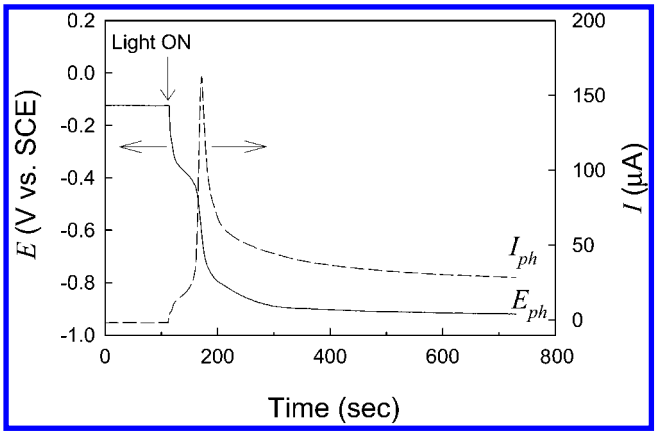

Figure 2. Temporal variation of the potential (E_{ph}) and current (I_{ph}) in the TiO_2−steel galvanic couple under illumination. Experimental conditions were 0.1 M formate (pH 7) in the photoanode cell (TiO_2), 0.05 M K_2CO_3 (pH 11) in the corrosion cell (steel), and 30-W UV illumination (130 $\mu W/cm^2$).

TABLE 1: Effects of Various Hole Scavengers (0.05 M) in the Photoanode Cell on E_{ph} (V vs SCE) and I_{ph} (μA)[a]

hole scavenger	E_{ph}[b]	I_{ph}[b]
water	−0.47	8.4
methanol	−0.62	19.2
ethanol	−0.59	17.9
2-propanol	−0.59	17.2
formate	−0.87	21.1
acetate	−0.48	13.1
citrate	−0.55	16.4
oxalate	−0.49	14.4

[a] Experimental conditions: 0.05 M K_2CO_3 (pH 11) in the corrosion cell; 30-W UV illumination. [b] Measured after 1 h of continuous illumination.

with an accompanying new potential and current for the couple. Figure 2 shows that the coupled potential under illumination (E_{ph}) immediately shifted to −0.85 to −0.9 V and that the photocurrent in the couple (I_{ph}) rose to a peak value within a minute or so and reached a steady state of ∼20 μA in a few minutes.

To reduce the charge−pair recombination and enhance the electron flow to the steel electrode, various hole scavengers were tested for their effects on E_{ph} and I_{ph} and are compared in Table 1. Formate showed the highest activity in changing both E_{ph} and I_{ph}, although others had comparable effects. The current-doubling effect with formate (reactions 1 and 2) could be responsible for the high activity. Even in the absence of an added electron donor (water only), appreciable values of E_{ph} and I_{ph} were attained. With the formate in the photoanode compartment, E_{ph} and I_{ph} remained constant under illumination up to ∼20 days, after which time E_{ph} shifted to less negative values because of the oxidative depletion of formate. Refilling the formate restored the E_{ph} values.

$$h_{vb}^{+} + HCOO^{-} \rightarrow HCOO\bullet \quad (1)$$

$$HCOO\bullet \rightarrow CO_2 + H^{+} + e^{-} \quad (2)$$

The effect of formate concentration was investigated. Figure 3a shows that both E_{ph} and I_{ph} rapidly changed with increasing concentration of formate and were saturated above 0.05 M. The effect of the TiO_2 coating thickness shown in Figure 3b also exhibited a similar trend of rapid change with increasing thickness and then saturation in both E_{ph} and I_{ph} above a thickness of ∼5 μm. The absorption of photons by the TiO_2 coating increases with the thickness and gets saturated when the coating is thicker than the light penetration depth. Although

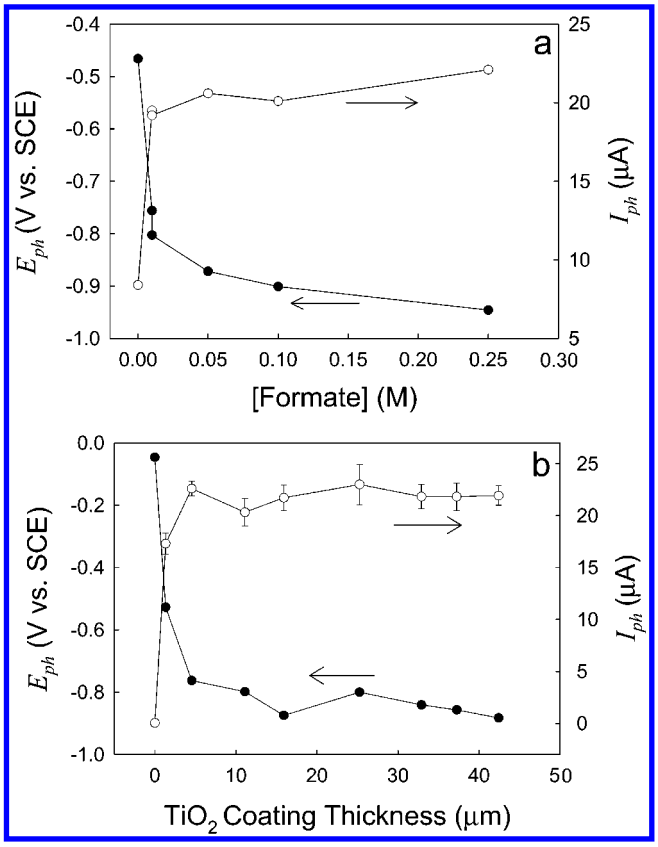

Figure 3. Variations of E_{ph} and I_{ph} in the TiO_2−steel galvanic couple as a function of (a) the formate concentration in the photoanode cell and (b) the thickness of the TiO_2 coating on ITO. The experimental conditions were 0.05 M K_2CO_3 (pH 11) in the corrosion cell, 0.1 M formate (pH 7) in the photoanode cell for (b), and 30-W UV illumination.

the intrinsic UV penetration depth into crystalline TiO_2 is within submicrometers,[12] the presence of voids within the coating usually makes the penetration depth much greater. The porosity of the TiO_2 coating made from the deposition of Degussa P25 suspension has been previously estimated to be 0.6 regardless of the coating thickness.[13] Because of this highly porous structure of the TiO_2 coating, E_{ph} and I_{ph} reached the saturation level at a much greater thickness than the intrinsic light penetration depth. This result might be compared with the finding that light (λ = 320 nm) incident on a TiO_2 colloidal particle was extinguished by 90% after traversing a distance of 0.39 μm.[2] In photoelectrochemical systems employing porous TiO_2 films, the optimal thickness has been reported to be 4∼15 μm,[14,15] which is consistent with this study. A typical TiO_2 coating thickness used in this study was ∼10 μm.

The relative electrode area in the couple of the photoanode and the steel cathode should be an important parameter as well. Figure 4 shows the effect of the cathode-to-anode area ratio (A_c/A_a) on the E_{ph} and on the anodic (J_a) or cathodic (J_c) current density ($J_a = I_{ph}/A_a$; $J_c = I_{ph}/A_c$). Upon increasing the area ratio, E_{ph} shifted to the positive direction. At low area ratios ($A_c/A_a < 0.5$), which was the usual condition in this work, the anodic current density (J_a) linearly increased with A_c/A_a, which implies that the photocurrent was controlled by cathodic limitation. The larger steel cathode area compared to the photoanode area provided more surface for the reduction reaction, and more photocurrent flowed. It will be further discussed in a later section how the cathodic conditions in the corrosion cell control the photocurrent in the TiO_2−steel electrode couple. At high area ratios ($A_c/A_a > 0.5$), however, J_a remained constant while J_c

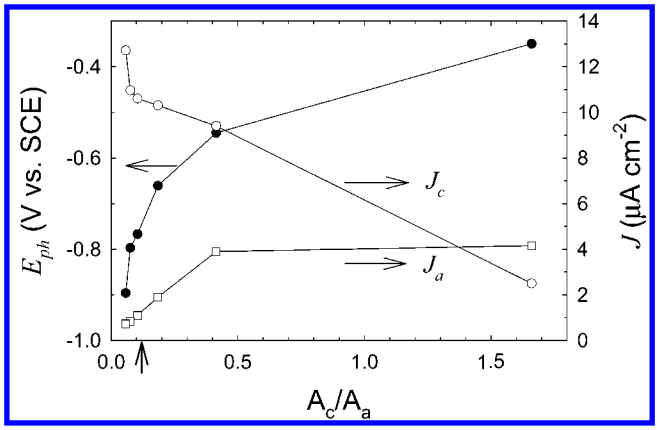

Figure 4. E_{ph} and the cathodic or anodic current density (J_c or J_a) as a function of the electrode area ratio (A_c/A_a). The area of the photoanode (A_a) was varied while the steel cathode area was fixed ($A_c = 1.66$ cm^2). All other data in this work were obtained at $A_c/A_a = 0.11$, which is indicated with an arrow on the abscissa.

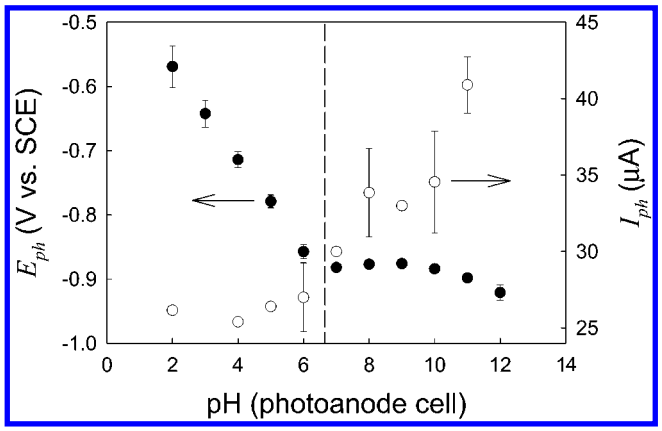

Figure 5. Variations of E_{ph} and I_{ph} as a function of the pH in the photoanode cell. The experimental conditions were 0.1 M formate in the photoanode cell, 0.05 M K_2CO_3 (pH 11) in the corrosion cell, and 30-W UV illumination.

steadily decreased, which indicates that the photocurrent was limited by the anodic condition (i.e., photon flux) in this region. A similar relationship between the cathode-to-anode area ratio and current densities was observed in a typical metal−metal galvanic couple.[16]

Figure 5 displays the variation of E_{ph} and I_{ph} as a function of pH in the photoanode compartment. The pH dependence can be clearly divided into two regions where the border line (dashed line in Figure 5) is around pH 6∼7. At pH < 7, E_{ph} shifted to negative values by about 70 mV with a 1 pH unit increase, which was mainly ascribed to the well-known Nernstian behavior of the TiO_2 flat-band potential.[12,17,18] Further increases of pH above ∼7 changed E_{ph} very little; it remained around −0.9 V. However, the pH dependence of I_{ph} showed the reverse trend to that of E_{ph}. Whereas I_{ph} remained constant in the region of pH < 7 where E_{ph} linearly changed, I_{ph} showed a near-linear increase with increasing pH above 7 where E_{ph} varied little. In view of the fact that the hole-scavenging efficiency of formate should be minimized at basic pH because of the electrostatic repulsion between the formate anion and the negatively charged TiO_2 surface, I_{ph} that was enhanced at alkaline conditions did not seem to be limited by the recombination process at the TiO_2 photoanode in this case. There should be other limiting parameters that affect I_{ph}. The lack of electron acceptors in the cathodic compartment could control the overall photocurrent. With the TiO_2 electrode at acidic pH and correspondingly less negative E_{ph} values, the dissolved oxygen, which has a limiting

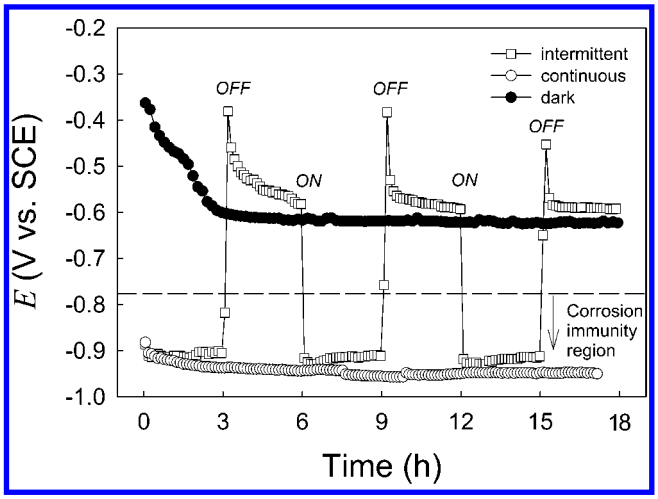

Figure 6. Potential changes in the TiO_2−steel galvanic couple under different illumination conditions of dark, continuous, and intermittent light. The experimental conditions consisted of the TiO_2 photoanode in formate-containing agar gel, 10 g/L NaCl solution (pH ∼ 7) in the corrosion cell, and 30-W UV illumination.

solubility (∼0.2 mM) in the ambient air, is the only electron acceptor (reaction 3) in the corrosion cell.

$$\begin{aligned} O_2 + H^+ + e^- &= HO_2 \\ HO_2 + H^+ + e^- &= H_2O_2 \\ H_2O_2 + H^+ + e^- &= H_2O + HO \\ HO + H^+ + e^- &= H_2O \\ \text{Overall: } O_2 + 4H^+ + 4e^- &= 2H_2O \end{aligned} \quad (3)$$

Therefore, I_{ph} is limited by the mass transfer rate of dissolved oxygen to the steel surface in this galvanic cell. However, when E_{ph} becomes more negative with a TiO_2 electrode at basic pH, water itself as well as oxygen can accept electrons from the steel electrode with increasing I_{ph}. In accordance with the argument, the onset potential of the photocurrent increase (in Figure 5) corresponded to the water reduction potential (reaction 4) in the cathodic compartment.

$$2H_2O + 2e^- = H_2 + 2OH^- \text{ (pH 11)} \quad E^\circ = -0.89 \text{ V}_{SCE} \quad (4)$$

Performance of the Photocathodic Metal Protection. The corrosion prevention of the steel connected to the TiO_2 photoanode was tested under continuous and intermittent illumination. The potential of the galvanic couple immediately responded to the presence and absence of light as shown in Figure 6. Under a 30-W black light, E_{ph} was maintained below −0.77 V_{SCE}, that is, in the corrosion immunity region.[10] Corrosion prevention under this condition was obvious enough to be detected visually. The shiny surface of the steel electrode remained intact in the corrosion electrolyte solution as long as it was connected to the photoanode whereas it quickly corroded and was covered by red-brown rust in the absence of light. The progress of corrosion under the different illumination conditions of Figure 6 is quantitatively compared by taking the Raman spectra of steel surfaces (Figure 7a). All the Raman peaks generated as a result of corrosion are ascribed to various phases of iron oxides.[19] The surface of the steel electrode that was connected to the continuously illuminated photoanode showed no sign of iron oxide formation whereas the dark control experiment produced a thick layer of iron oxide. The periodical

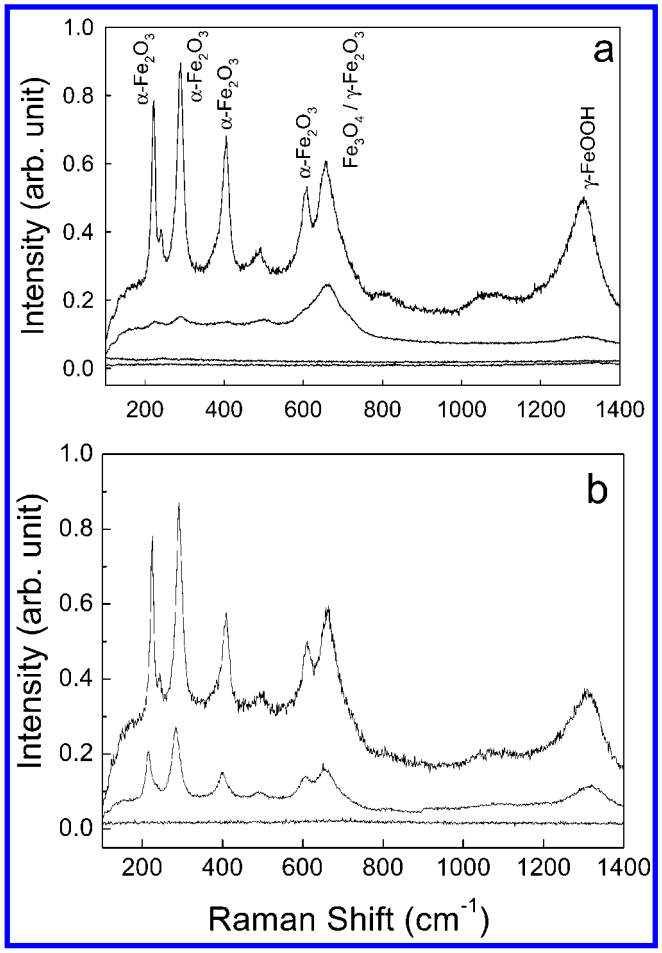

Figure 7. Raman spectra of the steel electrode surfaces that were corroded under different illumination conditions with the TiO_2 photoanode connected. (a) Under a 30-W black light (the condition of Figure 6), the data correspond to the following: (from bottom to top) initial steel surface, continuously illuminated (18 h), intermittently illuminated (9 h light + 9 h dark), and a dark control (18 h). (b) Under solar light and with the TiO_2 photoanode in formate-containing agar gel and 10 mM K_2CO_3 solution (pH 6.2) in the corrosion cell, the data correspond to the following: (from bottom to top) initial steel surface, illuminated in air (16 h day + 14 h night) and a control in the absence of the TiO_2 photoanode (30 h).

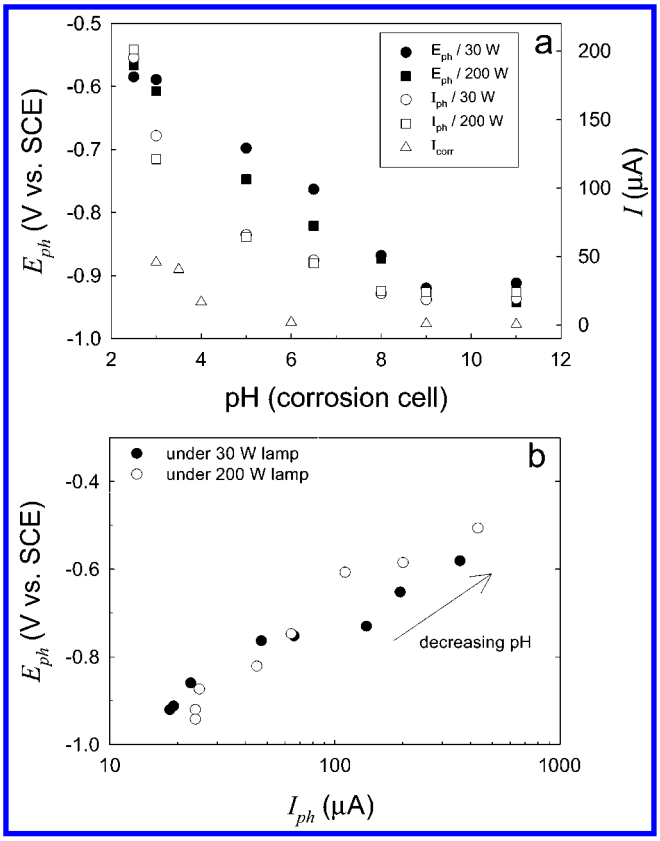

Figure 8. (a) Effect of pH in the corrosion cell on E_{ph}, I_{ph}, and I_{corr} under 30-W (130 μW/cm^2) or 200-W (1.54 mW/cm^2) illumination. (b) E_{ph} replotted as a function of I_{ph}. The experimental conditions consisted of the TiO_2 photoanode in formate-containing agar gel and 0.05 M K_2CO_3 in the corrosion cell.

illumination, however, did not completely inhibit the corrosion process as evidenced by an intermediate level of oxide peak intensity. The galvanic couple that was illuminated by sunlight in the open air experienced a moderate but lesser degree of corrosion than that of the control sample (Figure 7b) because the total corrosion time included both day and night.

Effects of Light Intensity and a Corrosion Environment. The photoinduced potentials and currents in the galvanic couple should be affected by many parameters. First of all, the pH effect on the corrosion of iron in aerated water is well-known. In the intermediate pH range of 4−10, the corrosion rate is nearly constant and is controlled by the diffusion of dissolved oxygen. At pH < 4, the corrosion rate rapidly increases because of the availability of H^+ for reduction whereas it becomes low above pH 10 because of the formation of the passive ferric oxide film.[10] Therefore, the pH in the corrosion cell should have a significant effect on the performance of this photocathodic system. Light intensity should be an important parameter as well. Figure 8a displays the pH dependences of E_{ph} and I_{ph} under the lower (30 W) or higher (200 W) light intensity and compares them with the dark corrosion current (I_{corr}). I_{ph} was closely correlated with I_{corr} whereas both I_{ph} and E_{ph} showed little dependence on light intensity (30 vs 200 W). I_{ph} ranged from 20 to 200 μA in the pH 2.5−11 region even under a constant light intensity. Although the present photocathodic system is essentially identical to a typical photoelectrochemical cell that converts light into electricity, where I_{ph} is proportional to light intensity,[20−22] it is clearly distinguished from the latter by the fact that its performance is mainly controlled by I_{corr}, not by light intensity as long as there are enough photons to compensate for the dark corrosion current. The steel could be protected from corrosion in the region of $I_{ph} > I_{corr}$ (pH 3−11) whereas the corrosion prevention is not sufficient in the region of $I_{ph} < I_{corr}$ (pH < 3, data not shown). Therefore, the conditions in the corrosion cell should be critical parameters affecting the design of the photoanode solar panel. With typical corrosion currents less than 10 μA (A_c = 1.66 cm^2) at pH > 5, I_{ph} of 15 μA that was obtained under UV intensity as low as 50 μW/cm^2 (10-W lamp) could match I_{corr}.

Cathodic Polarization in the TiO_2−Steel Couple. The polarization diagram in which the anodic and cathodic half-cell reactions are represented as a plot of E versus log I gives a quantitative assessment of the corrosion-rate inhibition caused by cathodic polarization.[10] As in a typical polarization diagram, E_{ph} and I_{ph} from Figure 8a are replotted in Figure 8b, which shows an approximately linear relationship between E_{ph} and log I_{ph}. As E_{ph} shifted to the positive direction under more corrosive environments, I_{ph} logarithmically increased.

The plot of E_{ph} versus I_{ph} is superimposed on the polarization diagram of iron in aerated water in Figure 9. The photocurrents in the photoanode (TiO_2)−cathode (steel) couple were greatly enhanced compared to the separate anodic current of iron (Fe $\rightarrow$ Fe^{2+} + $2e^-$). In this case, the photoanode supplied external

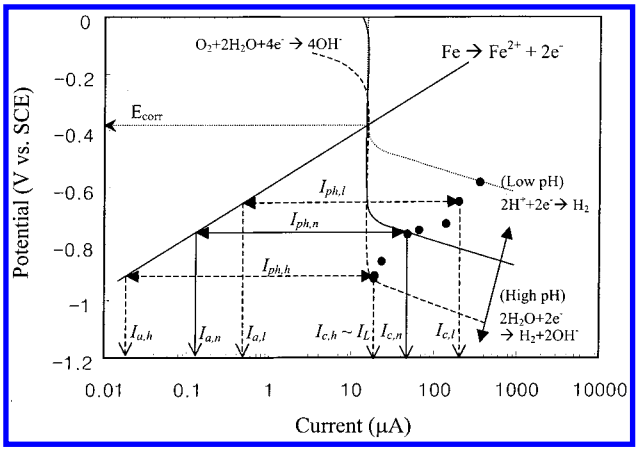

Figure 9. Polarization diagram for the photocathodic protection system with the galvanic couple of the TiO_2 photoanode and the steel electrode. The data points are from Figure 8b (30 W). The anodic polarization Tafel slope of the steel electrode was 0.1. Subscripts a and c refer to anodic and cathodic, respectively; l, n, and h refer to low, neutral, and high pH conditions, respectively.

current, resulting in the cathodic polarization of the steel electrode, which is essentially a variation of the impressed current cathodic protection. When a steel electrode connected to an illuminated photoanode is placed in aerated water of basic or neutral pH, electron transfer at the steel/solution interface is limited by the slow diffusion of dissolved oxygen, but a sufficient number of photogenerated electrons are transferred to the steel. Under this condition, the anodic current, I_a (i.e., corrosion rate) is greatly reduced from I_L to $I_{a,h}$ whereas the corresponding cathodic current ($I_{c,h}$) remains close to the limiting current (I_L).[10] The anodic and cathodic currents in Figure 9 refer to currents at low (I_l), neutral (I_n), and high (I_h) pH conditions. When the solution becomes more acidic, electron transfer at the steel/solution interface accelerates because of the proton reduction reaction ($2H^+ + 2e^- \rightarrow H_2$), which decreases the degree of cathodic polarization on the steel. As shown in Figure 9, decreasing pH increases both the anodic and cathodic current at the steel electrode ($I_{a,h} < I_{a,n} < I_{a,l}$; $I_{c,h} < I_{c,n} < I_{c,l}$) and the corresponding photocurrent ($I_{ph,h} < I_{ph,n} < I_{ph,l}$) as well.

Use of Water as a Hole Scavenger. The depletion of hole scavengers in the photoanode compartment with time seriously limits the practical application of this technology because the hole scavengers should be refilled periodically. Although water itself could serve as an alternative hole scavenger (reaction 5)[23] and should be the most durable and simple hole scavenging medium in a practical sense, it is usually not efficient in enhancing the CB electron-transfer rate on the TiO_2 surface.[24]

$$H_2O + h_{vb}^+ \rightarrow \bullet OH + H^+ \quad (5)$$

$$2(\bullet OH) \rightarrow H_2O_2 \quad (6)$$

As shown in Table 1, water without added hole scavengers was the least active in changing E_{ph} and I_{ph}. Nevertheless, the initial photocurrent of about 8 μA, which might be sufficient to counterbalance the corrosion current of steel, flowed. The photocurrent behavior of the TiO_2 photoanode cell, when using water as the hole scavenging medium, is shown in Figure 10. The corresponding values of E_{ph} and I_{ph} under four different conditions of water are compared in Table 2. The similar performance using the ZnO photoanode is compared with that of the TiO_2 photoanode in Figure 10 and Table 2. However, it should be noted that ZnO is relatively unstable with respect to its transformation to $Zn(OH)_2$ and may not serve as a good photoanode material from a practical point of view.

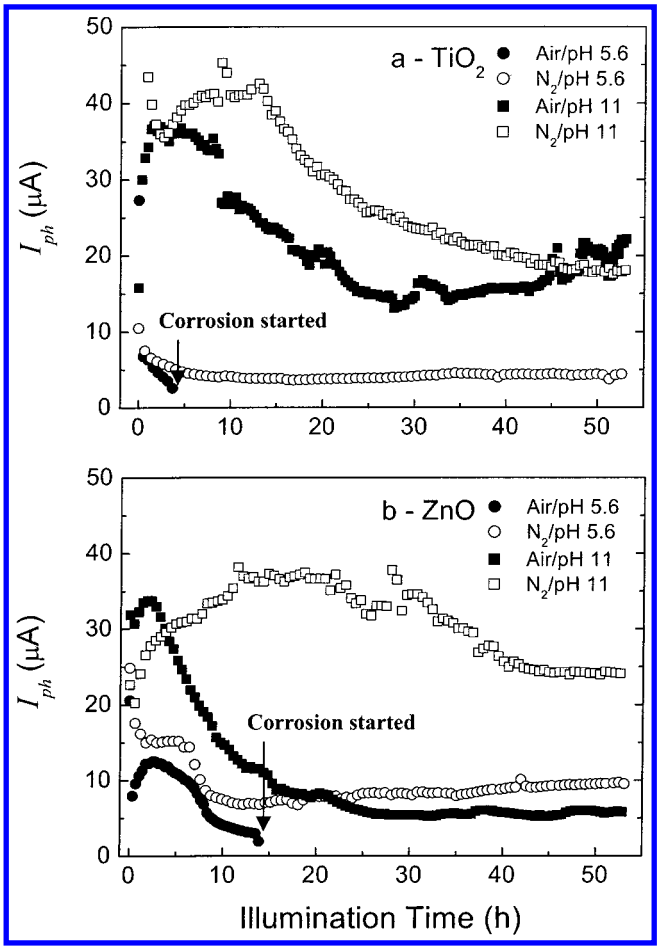

Figure 10. Variations of I_{ph} with illumination (30-W lamp: 130 μW/cm^2) time when only water was used as a hole scavenger in the (a) TiO_2 and (b) ZnO photoanode cell. Photocurrent behaviors under four different conditions of water (pH 5.6 vs 11; air-equilibrated vs N_2-saturated) are compared. The corrosion cell condition is air-equilibrated water (pH 5.6).

TABLE 2: Comparison of E_{ph} (V vs SCE) and I_{ph} (μA) under Different Conditions When Only Water Was Used as a Hole Scavenger in the TiO_2 or ZnO Photoanode Cell[a]

water (hole scavenger)	E_{ph}[b]	I_{ph}[b]
pH 5.6/air (TiO_2)	−0.39	6.5
pH 5.6/N_2 (TiO_2)	−0.48	7.0
pH 11/air (TiO_2)	−0.66	34.2
pH 11/N_2 (TiO_2)	−0.68	42.5
pH 5.6/air (ZnO)	−0.43	10.9
pH 5.6/N_2 (ZnO)	−0.45	16.8
pH 11/air (ZnO)	−0.59	32.6
pH 11/N_2 (ZnO)	−0.54	23.5

[a] Experimental conditions: air-equilibrated (pH 5.6) water in the corrosion cell; 30-W UV illumination. [b] Measured after 1 h of continuous illumination.

With air-equilibrated water (pH 5.6) in the photoanode cell, I_{ph} gradually decreased with illumination time, and the steel electrode began to corrode after 4.5 and 14 h with TiO_2 and ZnO photoanodes, respectively. When the dissolved oxygen in the TiO_2 (or ZnO) photoanode cell was removed by nitrogen purging, however, a constant level of photocurrent was maintained beyond 50 h, and there was no sign of corrosion. Dissolved oxygen molecules could intercept CB electrons at the semiconductor/water interface and subsequently decrease the electron flow to the steel electrode, which in turn reduces

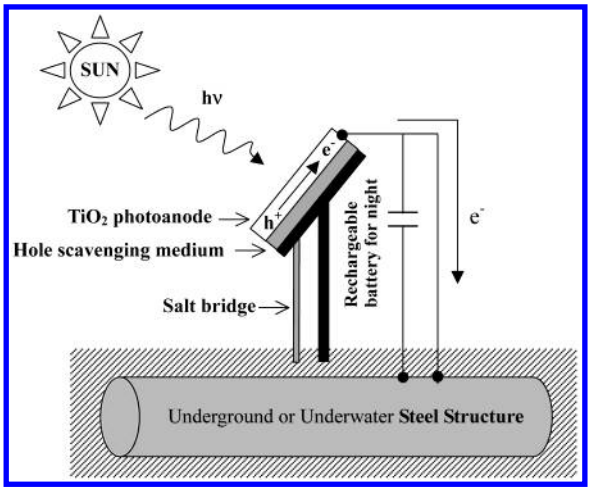

Figure 11. Schematic diagram of the proposed photocathodic metal protection system using a TiO_2 photoanode and solar light.

the corrosion inhibition effect. On the other hand, the negative effect of dissolved O_2 on corrosion prevention could be overcome by increasing pH as shown in Figure 10. At pH 11 (photoanode cell), the magnitude of I_{ph} was higher, and the corrosion of steel was not initiated either in the presence or absence of dissolved O_2. More negative E_{ph} and higher I_{ph} values at pH 11 (see Table 2) make the galvanic couple more corrosion-resistant, regardless of the presence of oxygen in the photoanode cell.

As a result of the oxidation of water (reactions 5, 6), H_2O_2 was produced in the deoxygenated photoanode cell. The H_2O_2 concentration in the TiO_2 photoanode cell after 50 h of continuous illumination was found to be 6 and 2 μM under pH 5.6/N_2 and pH 11/N_2 conditions, respectively. Much higher H_2O_2 concentrations were generated with the ZnO photoanode; these concentrations were measured to be 99 and 12 μM under pH 5.6/N_2 and pH 11/N_2 conditions (50 h of illumination), respectively. Kormann et al.[25] also observed that H_2O_2 could be photocatalytically produced via the oxidation of water in the absence of added electron donors and that its production quantum yield was much higher with ZnO than with TiO_2, mainly because of its lower photodegradation on ZnO and higher photodegradation on TiO_2. Although some of the H_2O_2 produced may have come from the reduction of residual O_2 that was not completely removed by nitrogen purging, the reductive path should be minor with $[O_2] < 10^{-5}$ M. The photogenerated H_2O_2 could be further oxidized to O_2 (reaction 7) or reduced back to H_2O (reaction 8) while maintaining a steady-state concentration.

$$H_2O_2 + 2h_{vb}^{+} \rightarrow O_2 + 2H^{+} \quad (7)$$

$$H_2O_2 + 2H^{+} + 2e_{cb}^{-} \rightarrow 2H_2O \quad (8)$$

Therefore, plain water could serve as a nondepleting hole scavenger in the TiO_2 (or ZnO) photoanode cell. The production of H_2O_2 in the corrosion cell that was connected to the TiO_2 or ZnO photoanode was much less ($\sim$1 μM).

Conclusions

A simple TiO_2-based photoelectrochemical system prevented steel corrosion by supplying photogenerated CB electrons to the steel electrode. The new photocathodic protection, which could be considered to be a variation of the impressed current method, verified the possibility of using solar light for metal corrosion inhibition. In view of the fact that conventional cathodic protection (sacrificial anode or impressed current method) requires the periodic replacement of buried sacrificial anodes or needs external power, the photoanode installed on the ground level under sunlight is easier to maintain.

A newly proposed photocathodic protection system is schematically depicted in Figure 11. Although the hole-scavenging medium that contains organic electron donors should be consumed under illumination, the use of plain water as a nondepleting hole-scavenging medium prevented corrosion, which made the semiconductor photoanode almost "nonsacrificial". The main technical barrier to be overcome in the practical development of this photocathodic protection is the absence of light at night. This problem could be solved by charging a battery by day and releasing the current at night, but with a higher cost. A novel approach using a TiO_2-WO_3 composite coating for light-energy storage[8] could be applied to the fabrication of the semiconductor photoanode and deserves further study.

Acknowledgment. This work was supported by the Korea Science and Engineering Foundation (KOSEF) through the Center for Integrated Molecular Systems and the Brain Korea 21 Project.

Note Added after ASAP Posting. This paper was posted ASAP 4/6/2002. Changes were made in eq 3 and text was added after eq 6 and before eq 7. The corrected version was posted 4/11/2002.

References and Notes

(1) Zou, Z.; Ye, J.; Sayama, K.; Arakawa, H. *Nature (London)* **2001**, *414*, 625.
(2) Hagfeldt, A.; Grätzel, M. *Chem. Rev.* **1995**, *95*, 49.
(3) (a) Hoffmann, M. R.; Martin, S. T.; Choi, W.; Bahnemann, D. W. *Chem. Rev.* **1995**, *95*, 69. (b) Choi, W.; Hong, S. J.; Chang, Y.-S.; Cho, Y. *Environ. Sci. Technol.* **2000**, *34*, 4810. (c) Cho, Y.; Choi, W.; Lee, C.-H.; Hyeon, T.; Lee, H.-I. *Environ. Sci. Technol.* **2001**, *35*, 966. (d) Cho, S.; Choi, W. *J. Photochem. Photobiol., A* **2001**, *143*, 221.
(4) Wang, R.; Hashimoto, K.; Fujishima, A.; Chikuni, M.; Kojima, E.; Kitamura, A.; Shimohigoshi, M.; Watanabe, T. *Nature (London)* **1997**, *388*, 431.
(5) Ha, H. Y.; Anderson, M. A. *J. Environ. Eng. (N.Y.)* **1996**, 217.
(6) Yuan, J.; Tsujikawa, S. *J. Electrochem. Soc.* **1995**, *142*, 3444.
(7) Ohko, Y.; Saitoh, S.; Tatsuma, T.; Fujishima, A. *J. Electrochem. Soc.* **2001**, *148*, B24.
(8) Tatsuma, T.; Saitoh, S.; Ohko, Y.; Fujishima, A. *Chem. Mater.* **2001**, *13*, 2838.
(9) Park, H.; Kim, K. Y.; Choi, W. *Chem. Commun.* **2001**, 281.
(10) Jones, D. A. *Principles and Prevention of Corrosion*, 9th ed.; Prentice Hall: Upper Saddle River, NJ, 1996.
(11) Mazellier, P.; Sulzberger, B. *Environ. Sci. Technol.* **2001**, *35*, 3314.
(12) Finklea, H. O. In *Semiconductor Electrodes*; Finklea, H. O., Ed.; Elsevier Science: New York, 1988; Chapter 2.
(13) Choi, W.; Ko, J. Y.; Park, H.; Chung, J. S. *Appl. Catal., B* **2001**, *31*, 209.
(14) Smestad, G.; Bigozzi, C.; Argazzi, R. *Sol. Energy Mater. Sol. Cells* **1994**, *32*, 259.
(15) Schlichthärl, G.; Huang, S. Y.; Sprange, J.; Frank, A. J. *J. Phys. Chem. B* **1997**, *101*, 8141.
(16) Liao, C.-M.; Wei, R. P. *Electrochim. Acta* **1999**, *45*, 881.
(17) Bard, A. J.; Bocarsly, A. B.; Fan, F. F.; Walton, E. G.; Wrighton, M. S. *J. Am. Chem. Soc.* **1980**, *102*, 3671.
(18) Bockris, J. O'M.; Khan, S. U. M. *Surface Electrochemistry*; Plenum Press: New York, 1993; Chapter 5.
(19) Oblonsky, L. J.; Devine, T. M. *Corros. Sci.* **1995**, *37*, 17.
(20) Fisher, A. C.; Peter, L. M.; Ponomarev, E. A.; Walker, A. B.; Wijayantha, K. G. U. *J. Phys. Chem. B* **2000**, *104*, 949.
(21) de Jongh, P. E.; Meulenkamp, E. A.; Vanmaekelbergh, D.; Kelly, J. J. *J. Phys. Chem. B* **2000**, *104*, 7686.
(22) Wang, H.; Lindgren, T.; He, J.; Hagfeldt, A.; Lindquist, S.-E. *J. Phys. Chem. B* **2000**, *104*, 5686.
(23) Yamakata, A.; Ishibashi, T.; Onishi, H. *J. Phys. Chem. B* **2001**, *105*, 7258.
(24) Choi, W.; Hoffmann, M. R. *Environ. Sci. Technol.* **1995**, *29*, 1646.
(25) Kormann, C.; Bahnemann, D. W.; Hoffmann, M. R. *Environ. Sci. Technol.* **1988**, *22*, 798.